

Measurement of D^0 - \bar{D}^0 mixing parameters using $D^0 \rightarrow K_S^0 \pi^+ \pi^-$ and $D^0 \rightarrow K_S^0 K^+ K^-$ decays

P. del Amo Sanchez,¹ J. P. Lees,¹ V. Poireau,¹ E. Prencipe,¹ V. Tisserand,¹ J. Garra Tico,² E. Grauges,² M. Martinelli^{ab,3} A. Palano^{ab,3} M. Pappagallo^{ab,3} G. Eigen,⁴ B. Stugu,⁴ L. Sun,⁴ M. Battaglia,⁵ D. N. Brown,⁵ B. Hooberman,⁵ L. T. Kerth,⁵ Yu. G. Kolomensky,⁵ G. Lynch,⁵ I. L. Osipenkov,⁵ T. Tanabe,⁵ C. M. Hawkes,⁶ A. T. Watson,⁶ H. Koch,⁷ T. Schroeder,⁷ D. J. Asgeirsson,⁸ C. Hearty,⁸ T. S. Mattison,⁸ J. A. McKenna,⁸ A. Khan,⁹ A. Randle-Conde,⁹ V. E. Blinov,¹⁰ A. R. Buzykaev,¹⁰ V. P. Druzhinin,¹⁰ V. B. Golubev,¹⁰ A. P. Onuchin,¹⁰ S. I. Serednyakov,¹⁰ Yu. I. Skovpen,¹⁰ E. P. Solodov,¹⁰ K. Yu. Todyshev,¹⁰ A. N. Yushkov,¹⁰ M. Bondioli,¹¹ S. Curry,¹¹ D. Kirkby,¹¹ A. J. Lankford,¹¹ M. Mandelkern,¹¹ E. C. Martin,¹¹ D. P. Stoker,¹¹ H. Atmacan,¹² J. W. Gary,¹² F. Liu,¹² O. Long,¹² G. M. Vitug,¹² C. Campagnari,¹³ T. M. Hong,¹³ D. Kovalskyi,¹³ J. D. Richman,¹³ A. M. Eisner,¹⁴ C. A. Heusch,¹⁴ J. Kroseberg,¹⁴ W. S. Lockman,¹⁴ A. J. Martinez,¹⁴ T. Schalk,¹⁴ B. A. Schumm,¹⁴ A. Seiden,¹⁴ L. O. Winstrom,¹⁴ C. H. Cheng,¹⁵ D. A. Doll,¹⁵ B. Echenard,¹⁵ D. G. Hitlin,¹⁵ P. Ongmongkolkul,¹⁵ F. C. Porter,¹⁵ A. Y. Rakitin,¹⁵ R. Andreassen,¹⁶ M. S. Dubrovin,¹⁶ G. Mancinelli,¹⁶ B. T. Meadows,¹⁶ M. D. Sokoloff,¹⁶ P. C. Bloom,¹⁷ W. T. Ford,¹⁷ A. Gaz,¹⁷ J. F. Hirschauer,¹⁷ M. Nagel,¹⁷ U. Nauenberg,¹⁷ J. G. Smith,¹⁷ S. R. Wagner,¹⁷ R. Ayad,^{18,*} W. H. Toki,¹⁸ T. M. Karbach,¹⁹ J. Merkel,¹⁹ A. Petzold,¹⁹ B. Spaan,¹⁹ K. Wacker,¹⁹ M. J. Kobel,²⁰ K. R. Schubert,²⁰ R. Schwierz,²⁰ D. Bernard,²¹ M. Verderi,²¹ P. J. Clark,²² S. Playfer,²² J. E. Watson,²² M. Andreotti^{ab,23} D. Bettoni^{a,23} C. Bozzi^{a,23} R. Calabrese^{ab,23} A. Cecchi^{ab,23} G. Cibinetto^{ab,23} E. Fioravanti^{ab,23} P. Franchini^{ab,23} E. Luppi^{ab,23} M. Munerato^{ab,23} M. Negrini^{ab,23} A. Petrella^{ab,23} L. Piemontese^{a,23} R. Baldini-Ferrolli,²⁴ A. Calcaterra,²⁴ R. de Sangro,²⁴ G. Finocchiaro,²⁴ M. Nicolaci,²⁴ S. Pacetti,²⁴ P. Patteri,²⁴ I. M. Peruzzi,^{24,†} M. Piccolo,²⁴ M. Rama,²⁴ A. Zallo,²⁴ R. Contri^{ab,25} E. Guido^{ab,25} M. Lo Vetere^{ab,25} M. R. Monge^{ab,25} S. Passaggio^{a,25} C. Patrignani^{ab,25} E. Robutti^{a,25} S. Tosi^{ab,25} B. Bhuyan,²⁶ C. L. Lee,²⁷ M. Morii,²⁷ A. Adametz,²⁸ J. Marks,²⁸ S. Schenk,²⁸ U. Uwer,²⁸ F. U. Bernlochner,²⁹ H. M. Lacker,²⁹ T. Lueck,²⁹ A. Volk,²⁹ P. D. Dauncey,³⁰ M. Tibbetts,³⁰ P. K. Behera,³¹ U. Mallik,³¹ C. Chen,³² J. Cochran,³² H. B. Crawley,³² L. Dong,³² W. T. Meyer,³² S. Prell,³² E. I. Rosenberg,³² A. E. Rubin,³² Y. Y. Gao,³³ A. V. Gritsan,³³ Z. J. Guo,³³ N. Arnaud,³⁴ M. Davier,³⁴ D. Derkach,³⁴ J. Firmino da Costa,³⁴ G. Grosdidier,³⁴ F. Le Diberder,³⁴ A. M. Lutz,³⁴ B. Malaescu,³⁴ A. Perez,³⁴ P. Roudeau,³⁴ M. H. Schune,³⁴ J. Serrano,³⁴ V. Sordini,^{34,‡} A. Stocchi,³⁴ L. Wang,³⁴ G. Wormser,³⁴ D. J. Lange,³⁵ D. M. Wright,³⁵ I. Bingham,³⁶ J. P. Burke,³⁶ C. A. Chavez,³⁶ J. P. Coleman,³⁶ J. R. Fry,³⁶ E. Gabathuler,³⁶ R. Gamet,³⁶ D. E. Hutchcroft,³⁶ D. J. Payne,³⁶ C. Touramanis,³⁶ A. J. Bevan,³⁷ F. Di Lodovico,³⁷ R. Sacco,³⁷ M. Sigamani,³⁷ G. Cowan,³⁸ S. Paramesvaran,³⁸ A. C. Wren,³⁸ D. N. Brown,³⁹ C. L. Davis,³⁹ A. G. Denig,⁴⁰ M. Fritsch,⁴⁰ W. Gradl,⁴⁰ A. Hafner,⁴⁰ K. E. Alwyn,⁴¹ D. Bailey,⁴¹ R. J. Barlow,⁴¹ G. Jackson,⁴¹ G. D. Lafferty,⁴¹ T. J. West,⁴¹ J. Anderson,⁴² R. Cenci,⁴² A. Jawahery,⁴² D. A. Roberts,⁴² G. Simi,⁴² J. M. Tuggle,⁴² C. Dallapiccola,⁴³ E. Salvati,⁴³ R. Cowan,⁴⁴ D. Dujmic,⁴⁴ P. H. Fisher,⁴⁴ G. Sciolla,⁴⁴ M. Zhao,⁴⁴ D. Lindemann,⁴⁵ P. M. Patel,⁴⁵ S. H. Robertson,⁴⁵ M. Schram,⁴⁵ P. Biassoni^{ab,46} A. Lazzaro^{ab,46} V. Lombardo^{a,46} F. Palombo^{ab,46} S. Stracka^{ab,46} L. Cremaldi,⁴⁷ R. Godang,^{47,§} R. Kroeger,⁴⁷ P. Sonnek,⁴⁷ D. J. Summers,⁴⁷ H. W. Zhao,⁴⁷ X. Nguyen,⁴⁸ M. Simard,⁴⁸ P. Taras,⁴⁸ G. De Nardo^{ab,49} D. Monorchio^{ab,49} G. Onorato^{ab,49} C. Sciacca^{ab,49} G. Raven,⁵⁰ H. L. Snoek,⁵⁰ C. P. Jessop,⁵¹ K. J. Knoepfel,⁵¹ J. M. LoSecco,⁵¹ W. F. Wang,⁵¹ L. A. Corwin,⁵² K. Honscheid,⁵² R. Kass,⁵² J. P. Morris,⁵² A. M. Rahimi,⁵² N. L. Blount,⁵³ J. Brau,⁵³ R. Frey,⁵³ O. Igonkina,⁵³ J. A. Kolb,⁵³ R. Rahmat,⁵³ N. B. Sinev,⁵³ D. Strom,⁵³ J. Strube,⁵³ E. Torrence,⁵³ G. Castelli^{ab,54} E. Feltresi^{ab,54} N. Gagliardi^{ab,54} M. Margoni^{ab,54} M. Morandin^{a,54} M. Posocco^{a,54} M. Rotondo^{a,54} F. Simonetto^{ab,54} R. Stroili^{ab,54} E. Ben-Haim,⁵⁵ G. R. Bonneaud,⁵⁵ H. Briand,⁵⁵ G. Calderini,⁵⁵ J. Chauveau,⁵⁵ O. Hamon,⁵⁵ Ph. Leruste,⁵⁵ G. Marchiori,⁵⁵ J. Ocariz,⁵⁵ J. Prendki,⁵⁵ S. Sitt,⁵⁵ M. Biasini^{ab,56} E. Manoni^{ab,56} C. Angelini^{ab,57} G. Batignani^{ab,57} S. Bettarini^{ab,57} M. Carpinelli^{ab,57,¶} G. Casarosa^{ab,57} A. Cervelli^{ab,57} F. Forti^{ab,57} M. A. Giorgi^{ab,57} A. Lusiani^{ac,57} N. Neri^{ab,57} E. Paoloni^{ab,57} G. Rizzo^{ab,57} J. J. Walsh^{a,57} D. Lopes Pegna,⁵⁸ C. Lu,⁵⁸ J. Olsen,⁵⁸ A. J. S. Smith,⁵⁸ A. V. Telnov,⁵⁸ F. Anulli^{a,59} E. Baracchini^{ab,59} G. Cavoto^{a,59} R. Faccini^{ab,59} F. Ferrarotto^{a,59} F. Ferroni^{ab,59} M. Gaspero^{ab,59} L. Li Gioi^{a,59} M. A. Mazzoni^{a,59} G. Piredda^{a,59} F. Renga^{ab,59} M. Ebert,⁶⁰ T. Hartmann,⁶⁰ T. Leddig,⁶⁰ H. Schröder,⁶⁰ R. Waldi,⁶⁰ T. Adye,⁶¹ B. Franek,⁶¹ E. O. Olaiya,⁶¹ F. F. Wilson,⁶¹ S. Emery,⁶² G. Hamel de Monchenault,⁶² G. Vasseur,⁶² Ch. Yèche,⁶² M. Zito,⁶² I. J. R. Aitchison,^{63,**}

M. T. Allen,⁶³ D. Aston,⁶³ D. J. Bard,⁶³ R. Bartoldus,⁶³ J. F. Benitez,⁶³ C. Cartaro,⁶³ M. R. Convery,⁶³ J. Dorfan,⁶³ G. P. Dubois-Felsmann,⁶³ W. Dunwoodie,⁶³ R. C. Field,⁶³ M. Franco Sevilla,⁶³ B. G. Fulsom,⁶³ A. M. Gabareen,⁶³ M. T. Graham,⁶³ P. Grenier,⁶³ C. Hast,⁶³ W. R. Innes,⁶³ M. H. Kelsey,⁶³ H. Kim,⁶³ P. Kim,⁶³ M. L. Kocian,⁶³ D. W. G. S. Leith,⁶³ S. Li,⁶³ B. Lindquist,⁶³ S. Luitz,⁶³ V. Luth,⁶³ H. L. Lynch,⁶³ D. B. MacFarlane,⁶³ H. Marsiske,⁶³ D. R. Muller,⁶³ H. Neal,⁶³ S. Nelson,⁶³ C. P. O'Grady,⁶³ I. Ofte,⁶³ M. Perl,⁶³ T. Pulliam,⁶³ B. N. Ratcliff,⁶³ A. Roodman,⁶³ A. A. Salnikov,⁶³ V. Santoro,⁶³ R. H. Schindler,⁶³ J. Schwiening,⁶³ A. Snyder,⁶³ D. Su,⁶³ M. K. Sullivan,⁶³ S. Sun,⁶³ K. Suzuki,⁶³ J. M. Thompson,⁶³ J. Va'vra,⁶³ A. P. Wagner,⁶³ M. Weaver,⁶³ C. A. West,⁶³ W. J. Wisniewski,⁶³ M. Wittgen,⁶³ D. H. Wright,⁶³ H. W. Wulsin,⁶³ A. K. Yarritu,⁶³ C. C. Young,⁶³ V. Ziegler,⁶³ X. R. Chen,⁶⁴ W. Park,⁶⁴ M. V. Purohit,⁶⁴ R. M. White,⁶⁴ J. R. Wilson,⁶⁴ S. J. Sekula,⁶⁵ M. Bellis,⁶⁶ P. R. Burchat,⁶⁶ A. J. Edwards,⁶⁶ T. S. Miyashita,⁶⁶ S. Ahmed,⁶⁷ M. S. Alam,⁶⁷ J. A. Ernst,⁶⁷ B. Pan,⁶⁷ M. A. Saeed,⁶⁷ S. B. Zain,⁶⁷ N. Guttman,⁶⁸ A. Soffer,⁶⁸ P. Lund,⁶⁹ S. M. Spanier,⁶⁹ R. Eckmann,⁷⁰ J. L. Ritchie,⁷⁰ A. M. Ruland,⁷⁰ C. J. Schilling,⁷⁰ R. F. Schwitters,⁷⁰ B. C. Wray,⁷⁰ J. M. Izen,⁷¹ X. C. Lou,⁷¹ F. Bianchi^{ab},⁷² D. Gamba^{ab},⁷² M. Pelliccioni^{ab},⁷² M. Bomben^{ab},⁷³ L. Lanceri^{ab},⁷³ L. Vitale^{ab},⁷³ N. Lopez-March,⁷⁴ F. Martinez-Vidal,⁷⁴ D. A. Milanés,⁷⁴ A. Oyanguren,⁷⁴ J. Albert,⁷⁵ Sw. Banerjee,⁷⁵ H. H. F. Choi,⁷⁵ K. Hamano,⁷⁵ G. J. King,⁷⁵ R. Kowalewski,⁷⁵ M. J. Lewczuk,⁷⁵ I. M. Nugent,⁷⁵ J. M. Roney,⁷⁵ R. J. Sobie,⁷⁵ T. J. Gershon,⁷⁶ P. F. Harrison,⁷⁶ J. Ilic,⁷⁶ T. E. Latham,⁷⁶ E. M. T. Puccio,⁷⁶ H. R. Band,⁷⁷ X. Chen,⁷⁷ S. Dasu,⁷⁷ K. T. Flood,⁷⁷ Y. Pan,⁷⁷ R. Prepost,⁷⁷ C. O. Vuosalo,⁷⁷ and S. L. Wu⁷⁷

(The BABAR Collaboration)

¹Laboratoire d'Annecy-le-Vieux de Physique des Particules (LAPP),
Université de Savoie, CNRS/IN2P3, F-74941 Annecy-Le-Vieux, France

²Universitat de Barcelona, Facultat de Física, Departament ECM, E-08028 Barcelona, Spain

³INFN Sezione di Bari^a; Dipartimento di Fisica, Università di Bari^b, I-70126 Bari, Italy

⁴University of Bergen, Institute of Physics, N-5007 Bergen, Norway

⁵Lawrence Berkeley National Laboratory and University of California, Berkeley, California 94720, USA

⁶University of Birmingham, Birmingham, B15 2TT, United Kingdom

⁷Ruhr Universität Bochum, Institut für Experimentalphysik 1, D-44780 Bochum, Germany

⁸University of British Columbia, Vancouver, British Columbia, Canada V6T 1Z1

⁹Brunel University, Uxbridge, Middlesex UB8 3PH, United Kingdom

¹⁰Budker Institute of Nuclear Physics, Novosibirsk 630090, Russia

¹¹University of California at Irvine, Irvine, California 92697, USA

¹²University of California at Riverside, Riverside, California 92521, USA

¹³University of California at Santa Barbara, Santa Barbara, California 93106, USA

¹⁴University of California at Santa Cruz, Institute for Particle Physics, Santa Cruz, California 95064, USA

¹⁵California Institute of Technology, Pasadena, California 91125, USA

¹⁶University of Cincinnati, Cincinnati, Ohio 45221, USA

¹⁷University of Colorado, Boulder, Colorado 80309, USA

¹⁸Colorado State University, Fort Collins, Colorado 80523, USA

¹⁹Technische Universität Dortmund, Fakultät Physik, D-44221 Dortmund, Germany

²⁰Technische Universität Dresden, Institut für Kern- und Teilchenphysik, D-01062 Dresden, Germany

²¹Laboratoire Leprince-Ringuet, CNRS/IN2P3, Ecole Polytechnique, F-91128 Palaiseau, France

²²University of Edinburgh, Edinburgh EH9 3JZ, United Kingdom

²³INFN Sezione di Ferrara^a; Dipartimento di Fisica, Università di Ferrara^b, I-44100 Ferrara, Italy

²⁴INFN Laboratori Nazionali di Frascati, I-00044 Frascati, Italy

²⁵INFN Sezione di Genova^a; Dipartimento di Fisica, Università di Genova^b, I-16146 Genova, Italy

²⁶Indian Institute of Technology Guwahati, Guwahati, Assam, 781 039, India

²⁷Harvard University, Cambridge, Massachusetts 02138, USA

²⁸Universität Heidelberg, Physikalisches Institut, Philosophenweg 12, D-69120 Heidelberg, Germany

²⁹Humboldt-Universität zu Berlin, Institut für Physik, Newtonstr. 15, D-12489 Berlin, Germany

³⁰Imperial College London, London, SW7 2AZ, United Kingdom

³¹University of Iowa, Iowa City, Iowa 52242, USA

³²Iowa State University, Ames, Iowa 50011-3160, USA

³³Johns Hopkins University, Baltimore, Maryland 21218, USA

³⁴Laboratoire de l'Accélérateur Linéaire, IN2P3/CNRS et Université Paris-Sud 11,

Centre Scientifique d'Orsay, B. P. 34, F-91898 Orsay Cedex, France

³⁵Lawrence Livermore National Laboratory, Livermore, California 94550, USA

³⁶University of Liverpool, Liverpool L69 7ZE, United Kingdom

³⁷Queen Mary, University of London, London, E1 4NS, United Kingdom

³⁸University of London, Royal Holloway and Bedford New College, Egham, Surrey TW20 0EX, United Kingdom

³⁹University of Louisville, Louisville, Kentucky 40292, USA

- ⁴⁰Johannes Gutenberg-Universität Mainz, Institut für Kernphysik, D-55099 Mainz, Germany
⁴¹University of Manchester, Manchester M13 9PL, United Kingdom
⁴²University of Maryland, College Park, Maryland 20742, USA
⁴³University of Massachusetts, Amherst, Massachusetts 01003, USA
⁴⁴Massachusetts Institute of Technology, Laboratory for Nuclear Science, Cambridge, Massachusetts 02139, USA
⁴⁵McGill University, Montréal, Québec, Canada H3A 2T8
⁴⁶INFN Sezione di Milano^a; Dipartimento di Fisica, Università di Milano^b, I-20133 Milano, Italy
⁴⁷University of Mississippi, University, Mississippi 38677, USA
⁴⁸Université de Montréal, Physique des Particules, Montréal, Québec, Canada H3C 3J7
⁴⁹INFN Sezione di Napoli^a; Dipartimento di Scienze Fisiche, Università di Napoli Federico II^b, I-80126 Napoli, Italy
⁵⁰NIKHEF, National Institute for Nuclear Physics and High Energy Physics, NL-1009 DB Amsterdam, The Netherlands
⁵¹University of Notre Dame, Notre Dame, Indiana 46556, USA
⁵²Ohio State University, Columbus, Ohio 43210, USA
⁵³University of Oregon, Eugene, Oregon 97403, USA
⁵⁴INFN Sezione di Padova^a; Dipartimento di Fisica, Università di Padova^b, I-35131 Padova, Italy
⁵⁵Laboratoire de Physique Nucléaire et de Hautes Energies, IN2P3/CNRS, Université Pierre et Marie Curie-Paris6, Université Denis Diderot-Paris7, F-75252 Paris, France
⁵⁶INFN Sezione di Perugia^a; Dipartimento di Fisica, Università di Perugia^b, I-06100 Perugia, Italy
⁵⁷INFN Sezione di Pisa^a; Dipartimento di Fisica, Università di Pisa^b; Scuola Normale Superiore di Pisa^c, I-56127 Pisa, Italy
⁵⁸Princeton University, Princeton, New Jersey 08544, USA
⁵⁹INFN Sezione di Roma^a; Dipartimento di Fisica, Università di Roma La Sapienza^b, I-00185 Roma, Italy
⁶⁰Universität Rostock, D-18051 Rostock, Germany
⁶¹Rutherford Appleton Laboratory, Chilton, Didcot, Oxon, OX11 0QX, United Kingdom
⁶²CEA, Irfu, SPP, Centre de Saclay, F-91191 Gif-sur-Yvette, France
⁶³SLAC National Accelerator Laboratory, Stanford, California 94309 USA
⁶⁴University of South Carolina, Columbia, South Carolina 29208, USA
⁶⁵Southern Methodist University, Dallas, Texas 75275, USA
⁶⁶Stanford University, Stanford, California 94305-4060, USA
⁶⁷State University of New York, Albany, New York 12222, USA
⁶⁸Tel Aviv University, School of Physics and Astronomy, Tel Aviv, 69978, Israel
⁶⁹University of Tennessee, Knoxville, Tennessee 37996, USA
⁷⁰University of Texas at Austin, Austin, Texas 78712, USA
⁷¹University of Texas at Dallas, Richardson, Texas 75083, USA
⁷²INFN Sezione di Torino^a; Dipartimento di Fisica Sperimentale, Università di Torino^b, I-10125 Torino, Italy
⁷³INFN Sezione di Trieste^a; Dipartimento di Fisica, Università di Trieste^b, I-34127 Trieste, Italy
⁷⁴IFIC, Universitat de Valencia-CSIC, E-46071 Valencia, Spain
⁷⁵University of Victoria, Victoria, British Columbia, Canada V8W 3P6
⁷⁶Department of Physics, University of Warwick, Coventry CV4 7AL, United Kingdom
⁷⁷University of Wisconsin, Madison, Wisconsin 53706, USA

(Dated: October 22, 2018)

We report a direct measurement of D^0 - \bar{D}^0 mixing parameters through a time-dependent amplitude analysis of the Dalitz plots of $D^0 \rightarrow K_S^0 \pi^+ \pi^-$ and, for the first time, $D^0 \rightarrow K_S^0 K^+ K^-$ decays. The low-momentum pion π_s^+ in the decay $D^{*+} \rightarrow D^0 \pi_s^+$ identifies the flavor of the neutral D meson at its production. Using 468.5 fb^{-1} of e^+e^- colliding-beam data recorded near $\sqrt{s} = 10.6 \text{ GeV}$ by the BABAR detector at the PEP-II asymmetric-energy collider at SLAC, we measure the mixing parameters $x = [1.6 \pm 2.3 \text{ (stat.)} \pm 1.2 \text{ (syst.)} \pm 0.8 \text{ (model)}] \times 10^{-3}$, and $y = [5.7 \pm 2.0 \text{ (stat.)} \pm 1.3 \text{ (syst.)} \pm 0.7 \text{ (model)}] \times 10^{-3}$. These results provide the best measurement to date of x and y . The knowledge of the value of x , in particular, is crucial for understanding the origin of mixing.

PACS numbers: 13.25.Ft, 11.30.Er, 12.15.Ff, 14.40.Lb

Particle-antiparticle mixing and CP violation (CPV) in the charm sector are predicted to be very small in the standard model (SM) [1–5]. Evidence for D^0 - \bar{D}^0 mixing has been found only recently [6–11] and CPV has not been observed. Although precise SM predictions for D^0 - \bar{D}^0 mixing are difficult to quantify, recent calculations of

the mixing parameters x and y allow for values as large as $\mathcal{O}(10^{-2})$ [1]. The analyses to date that have reported evidence for mixing have not been able to provide direct measurements of x and y . A time-dependent amplitude analysis of the Dalitz plot (DP) of D^0 mesons decaying into $K_S^0 \pi^+ \pi^-$ and $K_S^0 K^+ K^-$ self-conjugate final states

offers a unique way to access the mixing parameters x and y directly. In this Letter we study the time evolution of these three-body decays as a function of the position in the DP of squared invariant masses $s_+ = m^2(K_s^0 h^+)$, $s_- = m^2(K_s^0 h^-)$, where h represents π or K , and report the most precise single measurements of x and y to date. The knowledge of the value of x , in particular, is crucial for understanding the origin of mixing and for determining whether contributions beyond the SM are present.

We use the complete data sample of 468.5 fb⁻¹ recorded near $\sqrt{s} = 10.6$ GeV by the BABAR experiment [12] at the PEP-II asymmetric-energy e^+e^- collider. The flavor of the neutral D meson at production is identified through the charge of the π_s^+ (“slow pion”) produced in the decay $D^{*+} \rightarrow D^0 \pi_s^+$ [13]. The D^0 and \bar{D}^0 mesons evolve and decay as a mixture of the Hamiltonian eigenstates D_1 and D_2 , with masses and widths m_1 , Γ_1 and m_2 , Γ_2 , respectively. These mass eigenstates can then be written as linear combinations of flavor eigenstates, $|D_{1,2}\rangle = p|D^0\rangle \pm q|\bar{D}^0\rangle$, where $|p|^2 + |q|^2 = 1$. The mixing parameters are defined as $x = (m_1 - m_2)/\Gamma$ and $y = (\Gamma_1 - \Gamma_2)/2\Gamma$, where $\Gamma = (\Gamma_1 + \Gamma_2)/2$ is the average decay width.

Assuming no CPV in the decay, the relation $\bar{\mathcal{A}}(s_+, s_-) = \mathcal{A}(s_-, s_+)$ holds, where \mathcal{A} and $\bar{\mathcal{A}}$ are the decay amplitudes for a D^0 or a \bar{D}^0 into the final state $K_s^0 h^+ h^-$ as a function of the position in the DP. The time-dependent decay amplitude for a charm meson tagged at $t = 0$ as D^0 or \bar{D}^0 can then be written as

$$\begin{aligned} \mathcal{M}(s_+, s_-, t) &= \mathcal{A}(s_+, s_-)g_+(t) + \frac{q}{p}\mathcal{A}(s_-, s_+)g_-(t), \\ \bar{\mathcal{M}}(s_+, s_-, t) &= \frac{q}{p}\bar{\mathcal{A}}(s_+, s_-)g_+(t) + \bar{\mathcal{A}}(s_-, s_+)g_-(t), \end{aligned}$$

where $g_{\pm}(t) = 1/2 [e^{-i(m_1 - i\Gamma_1/2)t} \pm e^{-i(m_2 - i\Gamma_2/2)t}]$ and $q/p = 1$ if CP is conserved in the mixing amplitude. The decay rates for D^0 and \bar{D}^0 are obtained by squaring \mathcal{M} and $\bar{\mathcal{M}}$ respectively, and consist of a sum of terms depending on (s_+, s_-) and proportional to $\cosh(y\Gamma t)$, $\sinh(y\Gamma t)$, $\cos(x\Gamma t)$, and $\sin(x\Gamma t)$, all modulated by the exponential decay factor $e^{-\Gamma t}$. Assuming a model for $\mathcal{A}(s_+, s_-)$, it is possible to extract the mixing parameters x and y from the data, along with the amplitude model parameters and the proper-time resolution function. The variation of the distribution of the events in the DP as a function of the proper D^0 decay time is the signature of D^0 - \bar{D}^0 mixing. The sensitivity to x and y arises mostly from regions in the DP where Cabibbo-favored and doubly-Cabibbo-suppressed amplitudes interfere and from regions populated by CP eigenstates [14]. This method was pioneered by CLEO [15] and extended to a significantly larger data sample by Belle [16].

The D^0 candidates are reconstructed in the $K_s^0 \pi^+ \pi^-$ ($K_s^0 K^+ K^-$) final state by combining K_s^0 candidates with two oppositely-charged pions (kaons), with an invariant mass m_{D^0} between 1.824 and 1.904 GeV/ c^2 . In order to reduce combinatorial background and to remove D^0 can-

didates from B -meson decays, we require the momentum of the D^0 in the e^+e^- center-of-mass frame to be greater than 2.5 GeV/ c . The difference Δm between the D^{*+} and D^0 reconstructed invariant masses is required to satisfy $0.143 < \Delta m < 0.149$ GeV/ c^2 . Each pion (kaon) track is identified using a likelihood particle identification algorithm based on dE/dx ionization energy loss and Cherenkov angle measurements. The K_s^0 candidates are selected by pairing two oppositely-charged pions whose invariant mass is within 9 MeV/ c^2 of the nominal K_s^0 mass [17]. We require the cosine of the angle between the K_s^0 flight direction (defined by the K_s^0 production and decay vertices) and the K_s^0 momentum to be greater than 0.99, and a decay length projected along the K_s^0 momentum to be greater than 10 times its error. These selection criteria suppress to a negligible level the background from $D^0 \rightarrow \pi^+ \pi^- h^+ h^-$ decays. For each charged track we require a transverse momentum with respect to the beam axis to be greater than 100 MeV/ c , and for tracks from the D^0 decay we additionally require at least two hits in the two innermost layers of the silicon vertex tracker [12].

The D^0 proper time t , and its error σ_t , are obtained through a kinematic fit of the entire decay chain which constrains the K_s^0 and pion (kaon) tracks to originate from a common vertex and also requires the D^0 and the π_s^+ candidates to originate from a common vertex, constrained by the position and size of the e^+e^- interaction region. This reduces the contribution from $D^0 \rightarrow K_s^0 K_s^0$ decays (affecting only $K_s^0 \pi^+ \pi^-$) to 3% of the total background. We retain candidates for which the χ^2 probability of the fit is greater than 0.01%, $|t| < 6$ ps, and $\sigma_t < 1$ ps. The most probable value for σ_t is about 0.2 (0.3) ps for $K_s^0 \pi^+ \pi^-$ ($K_s^0 K^+ K^-$) signal candidates. For events where multiple D^{*+} candidates share one or more tracks, we keep the D^{*+} candidate with the highest χ^2 probability. After applying all selection criteria, we find 744 000 (96 000) $K_s^0 \pi^+ \pi^-$ ($K_s^0 K^+ K^-$) candidates. Their m_{D^0} and Δm distributions are shown in Fig. 1 and in [18].

The mixing parameters x and y are determined from an unbinned, extended maximum-likelihood fit to the $K_s^0 \pi^+ \pi^-$ and $K_s^0 K^+ K^-$ samples over the observables m_{D^0} , Δm , s_+ , s_- , t , and σ_t . First, the signal and background yields are determined from a fit to m_{D^0} and Δm distributions. For the subsequent fits, we restrict events to the signal region illustrated in Fig. 1, defined to lie within twice the measured resolution around the mean m_{D^0} and Δm values, and holding the signal and background yields fixed to their signal window rescaled values. In the mixing fit, the m_{D^0} and Δm shapes are excluded to minimize correlations with the rest of the observables. Our reference fit allows for mixing but assumes no CPV . We then allow for CPV as a cross-check of the mixing results. To avoid potential bias, the mixing results were examined only after the fitting and analysis procedures

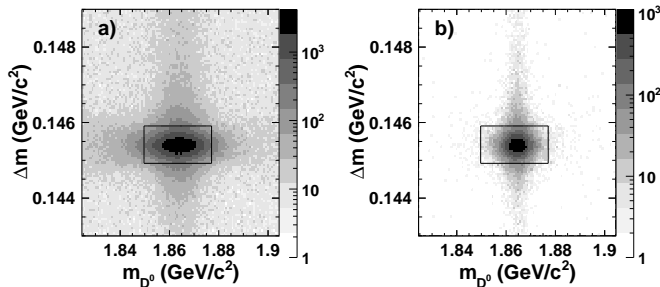


FIG. 1: Distributions of $m_{D^0} - \Delta m$ for (a) $K_s^0 \pi^+ \pi^-$ and (b) $K_s^0 K^+ K^-$ data after all selection criteria. The gray scale indicates the number of events per bin. The rectangles enclose the signal region.

were finalized.

For each fit stage, different sub-samples are characterized separately: $K_s^0 h^+ h^-$ signal, random π_s^+ , misreconstructed D^0 , $D^0 \rightarrow K_s^0 K_s^0$ events (for $K_s^0 \pi^+ \pi^-$ decays only), and combinatorial background. The random π_s^+ component describes correctly reconstructed D^0 decays combined with a random slow pion. Misreconstructed D^0 events have one or more D^0 decay products either missing or reconstructed with the wrong particle hypothesis. We account for $K_s^0 K_s^0$ background events since they exhibit a characteristic DP distribution and a signal-like shape in the variables t and σ_t . Combinatorial background events are those not described by the above components. The functional forms of the m_{D^0} , Δm probability density functions (PDFs) for the signal and background components are chosen based on studies performed on large Monte Carlo (MC) samples. These account for the observed correlations between Δm and m_{D^0} for signal and misreconstructed D^0 events. The PDF parameters are determined from two-dimensional likelihood fits to data over the full m_{D^0} and Δm region, or over dedicated sideband data samples. We find $540\,800 \pm 800$ ($79\,900 \pm 300$) signal events in the $K_s^0 \pi^+ \pi^-$ ($K_s^0 K^+ K^-$) signal region, with purities of 98.5% (99.2%), and reconstruction efficiencies of 14.4% (14.6%). Random π_s^+ , misreconstructed D^0 , and combinatorial background events account for 23% (53%), 52% (23%), and 22% (24%) of the total background. Projections of these fits and the contributions from the different background components can be found in [18].

The amplitudes $\mathcal{A}(s_+, s_-)$ are described by a coherent sum of quasi-two-body amplitudes [14, 19]. The dynamical properties of the P- and D-wave amplitudes are parameterized through intermediate resonances with mass-dependent relativistic Breit-Wigner (BW) or Gounaris-Sakurai (GS) propagators, Blatt-Weisskopf centrifugal barrier factors, and Zemach tensors for the angular distribution [19]. The $\pi\pi$ S-wave dynamics is described through a K-matrix formalism with the P-vector ap-

proximation and 5 poles [14, 20]. For the $K\pi$ S-wave we include a BW for the $K_0^*(1430)^\pm$ with a coherent non-resonant contribution parameterized by a scattering length and effective range similar to those used to describe $K\pi$ scattering data [18, 21]. For the $K\bar{K}$ S-wave, a coupled-channel BW is used for the $a_0(980)$ isovector with BWs for the $f_0(1370)$ and $a_0(1450)$ states.

We define PDFs to describe the dependence of the components in our event sample upon DP position (s_+, s_-) and upon decay time, t . For signal, $|\mathcal{M}|^2$ or $|\overline{\mathcal{M}}|^2$ is convolved with a proper-time resolution function different for $K_s^0 \pi^+ \pi^-$ and $K_s^0 K^+ K^-$ events with parameters determined by the mixing fit to the data. The resolution function is a sum of three Gaussians with one of the means allowed to differ from zero (the offset, t_0), and two of the widths proportional to σ_t . While t_0 does not depend sensitively on the DP position, the ability to reconstruct t varies as a function of (s_+, s_-). Hence, the observed distributions of σ_t in a number of DP regions are included in the signal PDF. We apply corrections for efficiency variations and neglect the invariant mass resolution across the DP. The time-dependent PDF for the small random π_s background component is described by an equal combination of D^0 and \bar{D}^0 signal events assuming no mixing, since the slow pion is positive or negative with approximately equal probability, and carries little weight in the vertex fit. The PDFs for misreconstructed D^0 events and combinatorial background are determined from m_{D^0} sideband samples. A non-parametric approach is used to construct the DP distributions, while the proper-time distributions are described by a sum of two Gaussian functions, one of which has a power-law tail to account for a small long-lived component. The background components containing real and misreconstructed D^0 decays have different σ_t distributions, which are determined from the signal and m_{D^0} sideband regions.

Results for our nominal mixing fit, in which D^0 and \bar{D}^0 samples from $K_s^0 \pi^+ \pi^-$ and $K_s^0 K^+ K^-$ channels are combined, are reported in Table I. The proper-time distributions with their fit projections are shown in Fig. 2. Additional fit results and projections can be found in [18]. We evaluate the amplitude model fit to the DP distribution with a χ^2 test with two-dimensional adaptive binning, and obtain $\chi^2 = 10\,429.2$ ($1\,511.2$) for $8\,626 - 41$ ($1\,195 - 17$) degrees of freedom (ndof), for $K_s^0 \pi^+ \pi^-$ ($K_s^0 K^+ K^-$). MC studies show that a significant contribution to these χ^2 values, $\Delta\chi^2/\text{ndof} \approx 0.16$, arises from imperfections in modeling experimental effects, mostly the efficiency variations at the boundaries of the DP and the invariant mass resolution. The fitted average lifetime $\tau = 1/\Gamma$ is found to be consistent with the world average lifetime [17], while t_0 is found to be 5.1 ± 0.8 fs (5.1 ± 2.2 fs) for the $K_s^0 \pi^+ \pi^-$ ($K_s^0 K^+ K^-$) mode, consistent with expectations from small misalignments in the detector [10].

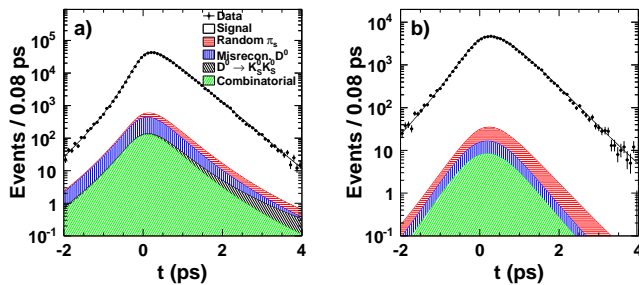


FIG. 2: (color online) Proper-time distributions for (a) $K_S^0 \pi^+ \pi^-$ and (b) $K_S^0 K^+ K^-$ data in the signal region with $-2 < t < 4$ ps (points). The curves show the fit projections for signal plus background (solid lines) and for different background components (shaded regions).

TABLE I: Results from the mixing fits. The first uncertainty is statistical, the second systematic and the third systematic from the amplitude model. For the nominal fit, the corresponding correlation coefficients between x and y are 3.5%, 16.0% and -2.7% , respectively.

Fit type	$x/10^{-3}$	$y/10^{-3}$
Nominal	$1.6 \pm 2.3 \pm 1.2 \pm 0.8$	$5.7 \pm 2.0 \pm 1.3 \pm 0.7$
$K_S^0 \pi^+ \pi^-$	2.6 ± 2.4	6.0 ± 2.1
$K_S^0 K^+ K^-$	-13.6 ± 9.2	4.4 ± 5.7
D^0	0.0 ± 3.3	5.5 ± 2.8
\bar{D}^0	3.3 ± 3.3	5.9 ± 2.8

A variety of studies using large MC samples with both parameterized and full detector simulations and data have been performed to validate the analysis method and fitting procedure and to check the consistency of the results. These studies demonstrate that the analysis correctly determines the mixing parameters with insignificant biases and well-behaved Gaussian errors. No significant variations of the mixing parameters are observed as a function of momentum, polar and azimuthal angles of the D^0 meson, and data taking period. Including the m_{D^0} , Δm PDFs in the mixing fit does not significantly change the values for x and y . The mixing fit has also been performed separately for the $K_S^0 \pi^+ \pi^-$ and $K_S^0 K^+ K^-$ data samples, and for D^0 and \bar{D}^0 decays, with the results listed in Table I. Fitting separately for D^0 and \bar{D}^0 provides a check against possible effects from CPV in mixing and in decay. Finally, if we fit the data forcing the decay amplitudes for D^0 and \bar{D}^0 to be the same (no direct CPV), but allowing their x and y values to differ, we find these values to be consistent (i.e., no evidence for CPV in mixing).

Systematic uncertainties arise from approximations in the modeling of experimental and selection criteria effects [18]. We account for variations in the signal and background yields, the efficiency variations across the

DP, the modeling of the DP and proper-time distributions for events containing misreconstructed D^0 decays, the misidentification of the D^0 flavor for signal and random π_s^+ events, potential effects due to mixing in the random π_s^+ background component, and PDF normalization. We also consider variations of the resolution function and σ_t PDFs, including alternatives to describe the correlation between σ_t and the DP position (e.g. neglecting the dependence of the σ_t distributions on the DP position entirely). The dominant sources of experimental systematic uncertainty are the limited statistics of full detector simulations (used to study potential biases due to the event selection, invariant mass resolution, residual correlations between the fit variables, and fitting procedure) and instrumental effects arising from the small misalignment of the detector. Effects from our selection criteria are estimated by varying the m_{D^0} , Δm , t , and σ_t requirements.

Assumptions in the amplitude models are also a source of systematic uncertainty [14, 18]. We use alternative models where the BW parameters are varied according to their uncertainties or changed to values measured by other experiments, the reference K-matrix solution [14] is replaced by other solutions [20], and the standard parameterizations are substituted by other related choices. These include replacing the GS by BW lineshapes, removing the mass dependence in the P-vector [22], changes in form factors such as variations in the Blatt-Weisskopf radius and the effect of evaluating the momentum of the spectator particle in the D^0 meson frame rather than in the resonance rest frame, and adopting a helicity formalism [19] to describe the angular dependence. Other models are built by removing or adding resonances with small or negligible fractions. The largest effect arises when the uncertainties in the amplitude model parameters obtained from the fit to the DP variables only [18] are propagated to the mixing fit. These uncertainties are dominated by the parameters related to the $K\pi$ S and P waves.

The mixing significance is evaluated by the variation of the negative log-likelihood ($-2\Delta \ln \mathcal{L}$) in the mixing parameter space. We account for the systematic uncertainties by approximating \mathcal{L} as a two-dimensional Gaussian with covariance matrix resulting from the sum of the corresponding statistical, systematic, and amplitude model matrices. Figure 3 shows the confidence-level (C.L.) contours in two dimensions (x and y) with systematic uncertainties included. The variation in $-2\Delta \ln \mathcal{L}$ for the no-mixing point is 5.6 units which corresponds to a C.L. equivalent to 1.9 standard deviations, including the systematic uncertainties.

In summary, we have directly measured the mixing parameters $x = [1.6 \pm 2.3$ (stat.) ± 1.2 (syst.) ± 0.8 (model)] $\times 10^{-3}$, and $y = [5.7 \pm 2.0$ (stat.) ± 1.3 (syst.) ± 0.7 (model)] $\times 10^{-3}$, using, for the first time, a combined analysis of $D^0 \rightarrow K_S^0 \pi^+ \pi^-$ and $D^0 \rightarrow$

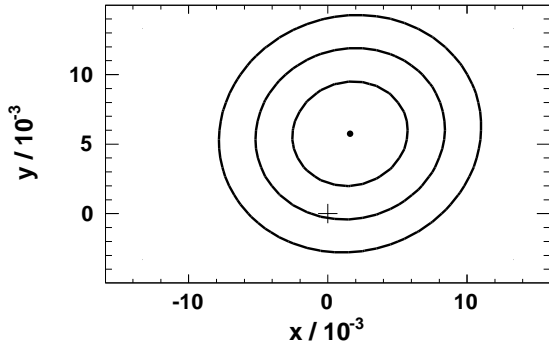


FIG. 3: Central value (point) and C.L. contours (including statistical, systematic and amplitude model uncertainties) in the x - y plane for C.L. = 68.3%, 95.4%, 99.7%. The no-mixing point is shown as a plus sign (+).

$K_s^0 K^+ K^-$ decays. These results are consistent with the previous similar measurements of $K_s^0 \pi^+ \pi^-$ alone [15, 16] and have improved precision. They disfavor the no-mixing hypothesis with a C.L. equivalent to 1.9 standard deviations and are in agreement with the range of SM predictions [1–5]. Our measurements favor lower values for x than for y , and lower x and y values (but still consistent) than those obtained when combining results from other D^0 decays [6–11, 23]. Adding our results to the combination of all previous analyses significantly improves our current knowledge of the mixing parameters x and y , whose average values change from $(9.8 \pm 2.5) \times 10^{-3}$ and $(8.3 \pm 1.6) \times 10^{-3}$ to $(5.9 \pm 2.0) \times 10^{-3}$ and $(8.0 \pm 1.3) \times 10^{-3}$, respectively [24].

We are grateful for the excellent luminosity and machine conditions provided by our PEP-II colleagues, and for the substantial dedicated effort from the computing organizations that support *BABAR*. The collaborating institutions wish to thank SLAC for its support and kind hospitality. This work is supported by DOE and NSF (USA), NSERC (Canada), CEA and CNRS-IN2P3 (France), BMBF and DFG (Germany), INFN (Italy), FOM (The Netherlands), NFR (Norway), MES (Russia), MICIIN (Spain), STFC (United Kingdom). Individuals have received support from the Marie Curie EIF (European Union), the A. P. Sloan Foundation (USA) and the Binational Science Foundation (USA-Israel).

- † Also with Università di Perugia, Dipartimento di Fisica, Perugia, Italy
‡ Also with Università di Roma La Sapienza, I-00185 Roma, Italy
§ Now at University of South Alabama, Mobile, Alabama 36688, USA
¶ Also with Università di Sassari, Sassari, Italy
** Also with University of Oxford, Theoretical Physics Department, Oxford, OX1 3NP, United Kingdom
- [1] A. A. Petrov, *Int. J. Mod. Phys. A* **21**, 5686 (2006).
[2] A. F. Falk, Y. Grossman, Z. Ligeti and A. A. Petrov, *Phys. Rev. D* **65**, 054034 (2002).
[3] I. I. Y. Bigi and N. G. Uraltsev, *Nucl. Phys. B* **592**, 92 (2001).
[4] L. Wolfenstein, *Phys. Lett. B* **164**, 170 (1985).
[5] A. F. Falk, Y. Grossman, Z. Ligeti, Y. Nir and A. A. Petrov, *Phys. Rev. D* **69**, 114021 (2004).
[6] B. Aubert *et al.* (*BABAR* Collaboration), *Phys. Rev. Lett.* **98**, 211802 (2007).
[7] M. Staric *et al.* (*Belle* Collaboration), *Phys. Rev. Lett.* **98**, 211803 (2007).
[8] T. Aaltonen *et al.* (*CDF* Collaboration), *Phys. Rev. Lett.* **100**, 121802 (2008).
[9] B. Aubert *et al.* (*BABAR* Collaboration), *Phys. Rev. D* **78**, 011105 (2008).
[10] B. Aubert *et al.* (*BABAR* Collaboration), *Phys. Rev. D* **80**, 071103 (2009).
[11] B. Aubert *et al.* (*BABAR* Collaboration), *Phys. Rev. Lett.* **103**, 211801 (2009).
[12] B. Aubert *et al.* (*BABAR* Collaboration), *Nucl. Instrum. Methods Phys. Res., Sect. A* **479**, 1 (2002).
[13] Reference to the charge-conjugate state is implied here and throughout the text unless otherwise stated.
[14] B. Aubert *et al.* (*BABAR* Collaboration), *Phys. Rev. D* **78**, 034023 (2008).
[15] D. M. Asner *et al.* (*CLEO* Collaboration), *Phys. Rev. D* **72**, 012001 (2005).
[16] L. M. Zhang *et al.* (*Belle* Collaboration), *Phys. Rev. Lett.* **99**, 131803 (2007).
[17] C. Amsler *et al.* (*Particle Data Group*), *Phys. Lett. B* **667**, 1 (2008).
[18] See supplementary material for additional mixing fit results and figures, and break-down of systematic uncertainties.
[19] See review on Dalitz plot analysis formalism in [17].
[20] V. V. Anisovich and A. V. Sarantsev, *Eur. Phys. Jour.* **A16**, 229 (2003).
[21] D. Aston *et al.*, *Nucl. Phys. B* **296**, 493 (1988); W. Dunwoodie, private communication.
[22] I. J. R. Aitchison, *Nucl. Phys. A* **189**, 417 (1972).
[23] J. L. Rosner *et al.* (*CLEO* Collaboration), *Phys. Rev. Lett.* **100**, 221801 (2008).
[24] A. Schwartz *et al.* (*Heavy Flavor Averaging Group*), <http://www.slac.stanford.edu/xorg/hfag/charm/index.html> (2010).

* Now at Temple University, Philadelphia, Pennsylvania 19122, USA

Measurement of D^0 - \bar{D}^0 mixing parameters using $D^0 \rightarrow K_S^0 \pi^+ \pi^-$ and $D^0 \rightarrow K_S^0 K^+ K^-$ decays

The BABAR Collaboration

The following includes supplementary material for the Electronic Physics Auxiliary Publication Service.

TABLE I: $D^0 \rightarrow K_S^0 \pi^+ \pi^-$ complex amplitudes, $\pi\pi$ P-vector and $K\pi$ S-wave parameters, and fit fractions, as obtained from the mixing fit. The $\pi\pi$ S-wave parameters β_5 , f_{14}^{prod} , and f_{15}^{prod} are fixed to zero due to the lack of sensitivity. We also report the mass and the width of the $K^*(892)^\mp$ resonance. Errors are statistical only. The fit fraction is defined as the integral over the entire DP of a single component divided by the coherent sum of all components. The sum of fit fractions is 103.3%. A detailed description of the parameters can be found elsewhere [14]. Equations (14) and (15) in [14] have been corrected as follows, $\mathcal{A}_{K\pi, L=0}(s) = T_{K\pi, L=0}(s)/\rho(s)$, where $\rho(s) = q/\sqrt{s}$ is the phase-space factor and $T_{K\pi, L=0}(s) = F \sin(\delta_F + \phi_F) e^{i(\delta_F + \phi_F)} + R \sin \delta_R e^{i(\delta_R + \phi_R)} e^{i2(\delta_F + \phi_F)}$, with $\tan \delta_R = M_{K_0^*(1430)} \Gamma_{K_0^*(1430)}(s)/(M_{K_0^*(1430)}^2 - s)$, $\cot \delta_F = 1/(aq) + rq/2$, s the invariant mass squared of the $K\pi$ system, and q the momentum of the kaon (or pion) in the $K\pi$ rest frame [21]. The symbol † indicates the parameters fixed in the mixing fit to the values extracted from a time-integrated DP fit to the same data. The results from this time-integrated DP fit for the amplitude model parameters agree within statistical errors with the results reported here.

Component	Amplitude	Phase (rad)	Fit fraction (%)
$K^*(892)^-$	1.735 ± 0.005	2.331 ± 0.004	57.0
$\rho(770)^0$	1	0	21.1
$K_0^*(1430)^-$	2.650 ± 0.015	1.497 ± 0.007	6.1
$K_2^*(1430)^-$	1.303 ± 0.013	2.498 ± 0.012	1.9
$\omega(782)$	0.0420 ± 0.0006	2.046 ± 0.014	0.6
$K^*(892)^+$	0.164 ± 0.003	-0.768 ± 0.019	0.6
$K^*(1680)^-$	0.90 ± 0.03	-2.97 ± 0.04	0.3
$f_2(1270)$	0.410 ± 0.013	2.88 ± 0.03	0.3
$K_0^*(1430)^+$	0.145 ± 0.014	1.78 ± 0.10	< 0.1
$K_2^*(1430)^+$	0.115 ± 0.013	2.69 ± 0.11	< 0.1
[$\pi\pi$ S-wave			15.4
β_1	5.54 ± 0.06	-0.054 ± 0.007	
β_2	15.64 ± 0.06	-3.125 ± 0.005	
β_3	44.6 ± 1.2	2.731 ± 0.015	
β_4	9.3 ± 0.2	2.30 ± 0.02	
f_{11}^{prod}	$11.43 \pm 0.11^\dagger$	$-0.005 \pm 0.009^\dagger$	
f_{12}^{prod}	$15.5 \pm 0.4^\dagger$	$-1.13 \pm 0.02^\dagger$	
f_{13}^{prod}	$7.0 \pm 0.7^\dagger$	$0.99 \pm 0.11^\dagger$	
	Parameter value		
[s_0^{prod}		-3.92637	
[$K\pi$ S-wave parameters			
$M_{K_0^*(1430)}$ (MeV/ c^2)		$1421.5 \pm 1.6^\dagger$	
$\Gamma_{K_0^*(1430)}$ (MeV/ c^2)		$247 \pm 3^\dagger$	
F		$0.62 \pm 0.04^\dagger$	
ϕ_F (rad)		$-0.100 \pm 0.010^\dagger$	
R		1	
ϕ_R (rad)		$1.10 \pm 0.02^\dagger$	
a (GeV/ c^{-1})		$0.224 \pm 0.003^\dagger$	
[r (GeV/ c^{-1})		$-15.01 \pm 0.13^\dagger$	
[$K^*(892)$ parameters			
$M_{K^*(892)}$ (MeV/ c^2)		$893.70 \pm 0.07^\dagger$	
[$\Gamma_{K^*(892)}$ (MeV/ c^2)		$46.74 \pm 0.15^\dagger$	

TABLE II: $D^0 \rightarrow K_S^0 K^+ K^-$ complex amplitudes and fit fractions, as obtained from the mixing fit. We also report the mass and the width of the $\phi(1020)$ resonance, and the $a_0(980)$ coupling constant to $K\bar{K}$ as determined from the fit. Errors are statistical only. The fit fraction is defined as the integral over the entire DP of a single component divided by the coherent sum of all components. The sum of fit fractions is 163.4%. A detailed description of the parameters can be found elsewhere [14]. The symbol † indicates the parameters fixed in the mixing fit to the values extracted from a time-integrated DP fit to the same data. The results from this time-integrated DP fit for the amplitude model parameters agree within statistical errors with the results reported here.

Component	Amplitude	Phase (rad)	Fit fraction (%)
$a_0(980)^0$	1	0	51.8
$\phi(1020)$	0.2313 ± 0.0011	-0.977 ± 0.008	44.1
$a_0(1450)^+$	$0.93 \pm 0.03^\dagger$	$1.66 \pm 0.07^\dagger$	25.6
$a_0(980)^+$	0.635 ± 0.006	-2.91 ± 0.02	19.5
$a_0(1450)^0$	$0.83 \pm 0.10^\dagger$	$-1.93 \pm 0.12^\dagger$	19.3
$f_0(1370)$	$0.16 \pm 0.05^\dagger$	$0.2 \pm 0.2^\dagger$	1.7
$f_2(1270)$	0.385 ± 0.015	0.06 ± 0.04	0.7
$a_0(980)^-$	0.125 ± 0.008	2.47 ± 0.04	0.7

$\lceil \phi(1020)$ and $a_0(980)$ parameters	Value
$M_{\phi(1020)}$ (MeV/ c^2)	$1019.55 \pm 0.02^\dagger$
$\Gamma_{\phi(1020)}$ (MeV/ c^2)	$4.60 \pm 0.04^\dagger$
$\lfloor g_{K\bar{K}}$ (MeV/ c^2)	$537 \pm 9^\dagger$

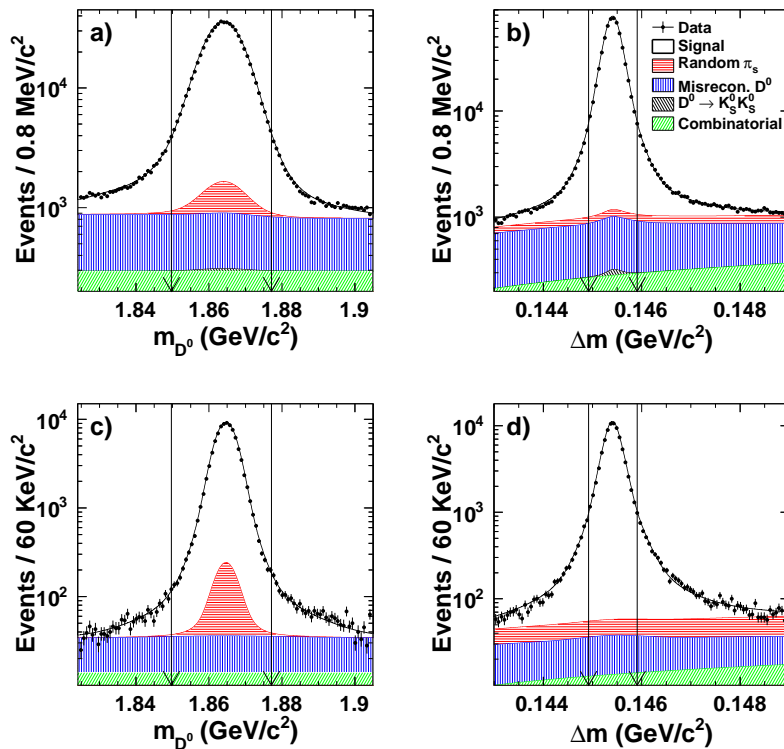


FIG. 1: (color online) Distributions of m_{D^0} and Δm for (a,b) $K_S^0 \pi^+ \pi^-$ and (c,d) $K_S^0 K^+ K^-$ data after all selection criteria (points). The curves superimposed represent the fit projections for signal plus background (solid lines) and for different background components (shaded regions). The arrows indicate the definition of the signal region.

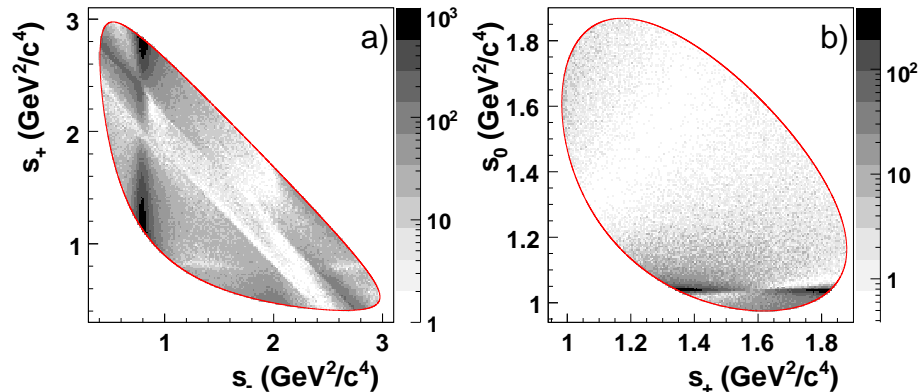


FIG. 2: DP distributions for (a) $D^0 \rightarrow K_S^0 \pi^+ \pi^-$ and (b) $D^0 \rightarrow K_S^0 K^+ K^-$ data after all selection criteria, in the signal region. The gray scale indicates the number of events per bin. The solid lines show the kinematic limits of the D^0 decay. The s_0 DP variable is defined as $s_0 = m^2(h^+ h^-)$. For \bar{D}^0 decays the variables s_- and s_+ are interchanged.

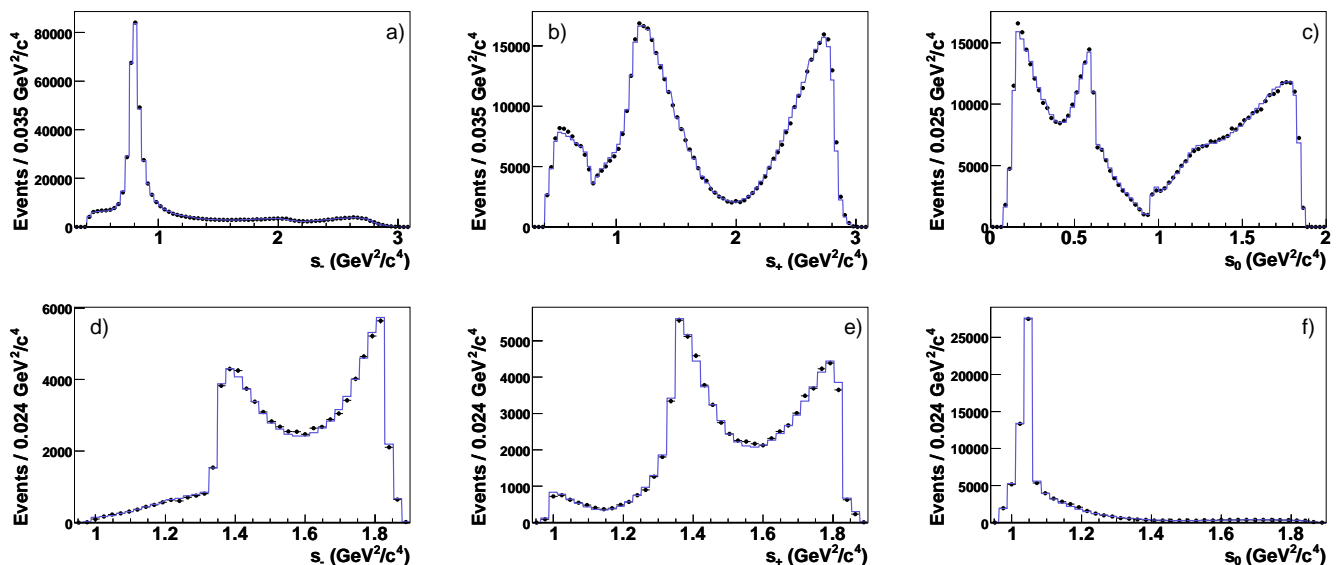


FIG. 3: DP projections for (a,b,c) $D^0 \rightarrow K_S^0 \pi^+ \pi^-$ and (d,e,f) $D^0 \rightarrow K_S^0 K^+ K^-$ data after all selection criteria, in the signal region (points). The histograms represent the mixing fit projections. For \bar{D}^0 decays the variables s_- and s_+ are interchanged.

TABLE III: Summary of the contributions to the experimental systematic uncertainty on the mixing parameters.

Source	$x/10^{-3}$	$y/10^{-3}$
Analysis biases and fitting procedure (Monte Carlo statistics)	0.75	0.66
Selection criteria	0.47	0.57
Signal and background yields	0.11	0.07
Efficiency variations across the DP	0.37	0.18
Modeling of the DP distributions for misreconstructed D^0 decays	0.33	0.14
Modeling of the proper-time distributions for signal and misreconstructed D^0 decays	0.13	0.13
Modeling of the proper-time error distributions for signal and misreconstructed D^0 decays	0.06	0.09
Misidentification of the D^0 flavor for signal and random π_s^+ events	0.49	0.40
Mixing in the random π_s^+ background component	0.10	0.08
PDF normalization	0.11	0.05
Misalignment of the detector	0.28	0.83
Total experimental systematic uncertainty	1.18	1.30

TABLE IV: Summary of the contributions to the D^0 decay amplitude model systematic uncertainty on the mixing parameters.

Source	$x/10^{-3}$	$y/10^{-3}$
Breit-Wigner parameters and alternative GS lineshapes	0.35	0.12
Alternative K-matrix solutions and P-vector parameterization	0.13	0.19
$K\pi$ S- and P-waves, and $\pi\pi$ S-wave parameters	0.68	0.53
Form factors	0.25	0.23
Angular dependence	0.05	0.17
Add/remove resonances	0.17	0.23
Total amplitude model systematic uncertainty	0.83	0.69